# RESEARCH ARTICLE

# Tumor Inhibition Effects and Mechanisms of *Angelica sinensis* and *Sophorae flavescentis ait* Decoction Combined with Cisplatin in Xenograft Mice

## De-Qi Yan, Yong-Qi Liu*, Ying-Dong Li, Dou Li, Xiao-Li Cheng, Zhi-Wei Wu

## Abstract

　　<u>Background</u>: To investigate tumor inhibition effects and mechanisms of *Angelica sinensis* and *Sophorae flavescentis* ait decoction (ASSF) combined with diamine-dichloroplatinum (DDP). <u>Materials and Methods</u>: Bodyweight, tumor inhibition rate and q value were calculated for single ASSF or ASSF combined with DDP on H22 carcinoma xenograft KM mice. Biochemical methods for serum LDH, AST, ALT, and AKP, ELISA method for serum HIF-1α, pathological assessemnt of thymus, immunohistochemistry detection of tumor tissue caspase3 and mutant p53 protein, and qRT-PCR detection of bax/ bcl-2 mRNA were applied. <u>Results</u>: Compared with DDP control group, the bodyweight increased in ASSF-DDP group (*p*<0.01). Tumor inhibition rates for DDP, ASSF, ASSF-DDP were 62.7%. 43.7% and 71.0% respectively, with a q value of 0.90. Compared with other groups, thymus of DDP control group had obvious pathological injury (*p*<0.01), serum LDH, AST, ALT, AKP increased significantly in DDP control group (*p*<0.01), while serum HIF-1α was increased in the model control group. Compared with this latter, the expression of mutant p53 protein and bcl-2 mRNA were decreased in all treatment groups (*p*<0.01), but there were no statistical difference between DDP control p and ASSF-DDP groups. The expression of caspase3 protein and bax mRNA was increased in all treatment groups, with statistical differences between the DDP and ASSF-DDP groups (*p*<0.01). <u>Conclusions</u>: ASSF can inhibit bodyweight decrease caused by DDP, can inhibit tumor growth synergistically with DDP mainly through increasing serum HIF-1α and pro-apoptotic molecules such as caspase 3 and bax, rather than through decreasing anti-apoptotic mutant p53 and bcl-2. ASSF can reduce DDP toxicity due to decreasing the release of LDH, AST, ALT, AKP into blood and enhancing thymus protection.

**Keywords:** *Angelica sinensis* - *Sophorae flavescentis* ait - decoction - H22 cells - tumor xenografts - DDP

## Introduction

　　Malignant tumors seriously endanger people's health, even life itself, cause physical and psychological pain and economic burden to the patients and their families. DDP (cis-diamine-dichloroplatinum II; C-DDP) is a kind of widely-used and highly effective anticancer agent, also used in anti-cancer experiment as positive control drug. However, the risk of its side effects and the resistance of cancer cells to it (Yu et al., 2012) frequently interrupt the use of higher doses that could maximize its anti-neoplastic effects.

　　In traditional Chinese medicine, the concept of malignant tumor belongs to the category of lumps resulted from blood stasis which then causes the defense system to become weak in overseeing the internal environment. *Angelica sinensis* and *Sophorae flavescentis* pill was first seen in Yizongjinjian. The prescription pill consists of *Angelica sinensis* and *Radix Sophora flavescens*, has the functions of nourishing the blood and making blood

peaceful, clearing internal heat and drying dampness, melting phlegm and scattering clot. Radix *Sophora flavescens* combined with *Angelica sinensis* is commonly used to treat skin disease with heat and dampness (Chen et al., 2013; Jin et al., 2013). When the cancer patients are in a state of internal stasis caused by heat and dampness, ASSF can be applied and get good effects. A lot of studies showed that some chemical composition in Radix *Sophora flavescens* was able to inhibit tumor cells *in vitro* (Zhang et al., 2012; Pu et al., 2013).

　　Hypoxia is a very common phenomenon in solid tumors and leads to aggressive phenotype and treatment failure. Hypoxia-inducible factor 1α (HIF-1α) regulates more than 5% of total human genes, Overexpression of HIF-1α is detected in many kinds of cancers via different kinds of mechanisms, including decreased oxygen concentration, hyperactivation of protein kinase signaling pathways, mutant oncogene activation, function loss of tumor suppressor gene, etc. Genes regulated by HIF-1α involve in many pathological processes such as drug

*Gansu Traditional Chinese Medicine College, Lanzhou, China  *For correspondence: yandq693@163.com, liuyongqi73@163.com*

efflux, metabolic switch, cell proliferation, angiogenesis, especially anti-apoptosis, metastasis and differentiation (Lee et al., 2014), which ultimately leads to drug resistance and tumor growth. Novel strategies have been developed to inhibit HIF activity in targeting hypoxic tumors. HIF-1α protein is often over-expressed in multiple types of human cancer and the major cause of resistance to drugs and radiation, involved in hypoxia-induced tumor progression and chemoresistance (Iovine et al., 2014).

This subject discussed the actual effect of ASSF to inhibit tumor growth, to reduce the side effect of DDP and increase its anti-tumor effect, also revealed the influence of ASSF on serum LDH, AST, ALT, AKP, and HIF-1α, and some apoptotic mechanism, in order to provide experimental basis for the clinical application of ASSF decoction united with DDP to treat cancer disease.

## Materials and Methods

*Experimental animals and facility*

SPF Kunming mice, half male and half female, 6-8 weeks, 20-22g, provided by the SPF animal experimental center of Gansu College of Traditional Chinese Medicine; SPF animal experimental facility NO.: SYXK (GAN) 2012-0001; Animal Certificate No.: SCXK (GAN) 2012 - 0001.

*Cell lines*

H22 liver cancer strain preserved in Institute of integrative medicine of Gansu College of Traditional Chinese Medicine.

*Herbs and reagents*

DDP injection, 10mg/bottle, China Qilu Drug Producing Co. Ltd., lot: 201002CF; Angelica sinensis came from Min county of Gansu in China. Radix Sophorae flavescentis was identified as good product according to China medicine dictionary by two experts. LDH (Nanjing Jiancheng Bio-engineering company, 20121011); AKP (Nanjing Jiancheng Bio-engineering company, 20121024); AST (Nanjing Jiancheng Bio-engineering company, A059-1); ALT (Nanjing Jiancheng Bio-engineering company, C009-1); HIF-1α (Shanghai Yuanye Bio-tech company, 201002CF ); Rabbit anti-p53 (Zhongsajinqiao cooperation, D1112); Rabbit anti-caspase 3 (Zhongsajinqiao cooperation, H1712); SV total RNA Isolation System (promega coporation, 0000014521). Transcriptor High Fidelity cDNA Synthesis Kit (Roche Applied Science, Indianapolis, IN, USA), Taq DNA polymerase (Violet, Taiwan).

*Instruments*

$CO_2$ incubator (NAPCO France), SW-CJ-IF super clean bench (China Suzhou purification equipment factory), electronic balance (LD100001, China Dragon Electronics Co. Ltd.), A0-820 rotary microtome (America Scientific Instruments), Bx53 inverted fluorescence microscope (Japan, OLYMPUS), Cellsense camera software. 0-150 mm electronic digital caliper (China Xuehuagongliang tool coporation). Stratagene Robocycler Gradient 96 (Stratagene, La Jolla, CA, USA).

*Preparation of ASSF*

Put 7.5g Angelica sinensis and 15.0g Sophora flavescens into the clay-made medicine pot. Add 250mL distilled water to immerse the herbs for 30min, then boil for 1h. Pour the boiled liquid into a cup. Add another 250mL distilled water into the clay medicine pot immersing for 30min, boiling 1h. Pour the boiled liquid into the above cup. Heat the mixed liquid in 70°Cwater bath to 50mL, for gavages on the same day. Drug concentration calculated according to crude herb was 0.45g/mL.

*Preparation of DDP solution*

Use 50mL physiological saline to wash 10mg DDP bottle and get 10mg/50mL DDP solution, which can be used for 5kg mice, the dosage being 2.0 mg/kg.

*Preparation of animal model*

174 KM mice were fed for 4 days to adapt the new environment. 12 female and 12 male mice were randomly selected into normal control group. The remaining mice were used for modeling. Inoculate 0.1 mL$^{-1}$ suspension with 105 H22 cancer cells into the subcutaneous right armpit of the ungrouped KM mice in the SPF animal laboratory. To observe the tumor growth of the mice inoculated with H22 cell during 5-7 days after inoculation. On the 7th day after inoculation, the nodules near the inoculation site could be palpable, 5 female and 5 male mice were randomly selected for pathological examination of nodules. All the 10 nodules diagnosed as tumor tissue could suggest that inoculation modeling was successful.

*Model animal grouping and treatment*

On the eighth day from inoculation, eliminate the mice with too small, or too large nodules, randomly select 48 female mice and 48 male mice with nodules of moderate size, and randomize them into model control group, DDP control group, ASSF group and ASSF-DDP group, 12 female and 12 male mice in each group. Weight the mice after grouping, gavage 0.4ml/20g and intraperitoneally inject 0.2ml/20g physiological saline respectively into the model control group; gavage 0.4ml/20g physiological saline and intraperitoneally inject 0.2ml/20g DDP solution respectively into DDP control group; gavage 0.4ml/20g ASSF and intraperitoneally inject 0.2ml/20g physiological saline respectively into ASSF group; gavage 0.4ml/20g ASSF and intraperitoneally inject 0.2ml/20g DDP solution into ASSF -DDPgroup. The administration of medicine consists for 14 days, once a day.

*Tumor inhibition rate and q value*

Tumor inhibition rate (%)=(mean tumor weight of model control group - mean tumor weight of experiment group) /mean tumor weight of model control group. q value can be used to determine the type of combined effect of ASSF decoction and DDP. q=EAB/ (EA+ EB -EA *EB) . Where EA is the tumor inhibition rate of ASSF decoction group, EB the tumor inhibition rate of DDP group, EAB is the tumor inhibition rate of ASSF-DDPgroup. q<0.85 means antagonist, q between 0.85~1.15 means additive, q>1.15 means synergism (Liu et al., 2011).

*Preparation and observation of pathological sections*

Acquisition and fixation of the tissue: 8 male and 8 female mice in each group were randomly selected to isolate thymus. Thymus were fixed in 4% poly formaldehyde over16h.

Tissue washing, dehydration, transparency, immersing and burying with paraffin: Tissue fixed for enough time was taken out. Rinse 20min with flowing tap water. Wash out poly formaldehyde, followed by 75% alcohol 1h →85% alcohol over night→ 95% alcohol I 35min → 95% alcohol II 35min→ 100% alcohol I 35min → 100% alcohol II 30min for alcohol concentration gradient dehydration, transparent through dimethylbenzene xylene I 35min →dimethylbenzene xylene II 30min, then paraffin I 2h →paraffin II 2h for osmosis, finally embedded in paraffin.

Section cutting, pasting, staining, closing: Cut paraffin-embedded tissue blocks into 4μm thick sections.Gently spread on the 43°C surface of water, flattening it on the middle of a slide. Remove the water from slides and put it in an incubator chamber at 63°C baking for 20 minutes. Remove the interstitial paraffin wax. According to hematoxylin eosin staining method, dewax, remove benzene, rehydrate, dye, dehydrate, make transparency, and finally close the sections.

Observation and scoring method of pathologic sections: Observe HE pathological sections by inverted fluorescence microscope which magnify the object to 10×40 times, using Cellsense software to acquire picture. Three pathologists respectively select 5 typical visual field for each section, independently grade the picture according to the following standards. The average grading value of each section was calculated according to 15 typical field grading from three experts. The number of different grading values of 16 sections of each group was used in rank sum test analysis.

Observe thymus cells and reticular cells of thymus cortex and medulla of each group, and give them scores in accordance with the thymus cell numbers. 0: normal number of thymocytes. 1: less number of thymocytes than normal group. 2: a serious lack of thymus cells compared with normal group.

*Detection of serum LDH, AST, ALT, AKP and HIF-1α*

The blood were collected through eye socket and centrifuged to acquire serum for biochemical detection of LDH, AST, ALT, AKP and ELISA method detection of HIF-1α.

*Detection of mutant p53 and caspase-3 protein expression in the tumor tissue by immunohistochemistry*

5 male and 5 female mice in each tumor-bearing group were randomly selected to isolate tumor. The tumors were cut into 1.0cm×1.0cm×0.3cm pieces, fixed in 4% poly formaldehyde over 16h., processed and embedded in paraffin, then made into slices. P53 and caspase-3 protein expression were detected by immunohistochemistry according to product instruction. Dewax sections in xylene, restore the antigen by microwaving in 0.01 M sodium citrate buffer pH 6.0. Incubate slices with 3% $H_2O_2$ for 8 min. Wash 3 times with PBS for 3 min each time. Add agent A and incubate for 12 min at room temperature, then let agent A flow out. Add diluted Rabbit anti-p53 (FL-393) or Rabbit anti-caspase-3 (H277) and incubate for 2.5h at 37°C. Wash with PBS 3 times for 3min each time. Add agent B and incubate for 12 min at 37°C. Add agent C and incubate for 12 min at 37°C. Wash with PBS 3 times for 3min each time. Immerse the slices in diaminobenzidine hydrochloride (DAB). Wash the slices with tap water then mount them.

The mean density and mean grey scale of mutant p53 and caspase-3 slices were calculated by Image-Pro Plus 5.1 (USA) image analysis software. Each group was measured 10 sections representative for 10 tumors respectively.

*Detection of bcl-2 and bax mRNA expression in the tumor tissue by qRT-PCR*

10 tumors from 5 male and 5 female mice in each group were stored in liquid nitrogen. Homogenize tumor tissue with a homogenizer respectively. Total RNA was extracted from the homogenate by SV total RNA Isolation System(lot: 0000014521, promega coporation). The mRNA was then reversely transcribed into cDNA by Transcriptor High Fidelity cDNA Synthesis Kit (Roche Applied Science, Indianapolis, IN, USA). The cDNA was used as a template for quantitative real-time PCR analysis. Sequences for primers were obtained from Genbank. Primers were designed using Primer 5 and synthesized at BGI Tech (Shenzhen, China) (Table 1). For qRT-PCR reactions, 25 μL mixtures were made by using SYBR Premix Ex TaqTMII (DRR820A, Takara, Japanese), containing 12.5 μL Tli RNaseH Plus, 1.0 μL of sense and 1.0 μL of antisense primers, 8.5 μL RNAase-free water and 2μL cDNA. Reaction conditions were set to 3 min at 95°C (pre-degeneration), 10 s at 95°C (degeneration) and 30 s at Tm of a specific primer pair (annealing) followed 72°C for 10 s (extension) for 44 cycle in Thermal Cycler (C1000, BIO RAD, USA). mRNA expression was analyzed for bcl-2 and bax genes, and β-Actin was used for internal control gene. With 2-ΔΔCt assay, the results were analyzed.

*Statistical analysis*

Bodyweight, tumor weight , tumor volume of experimental data and tumor cell mitosis , mean density and mean grey scale of mutant p53 and caspase 3 can be expressed with ($\bar{x}$±s) and analyzed with SPSS17.0 statistical software for single factor analysis of variance. The pathological grade data can be scored according to above standards and analyzed by SPSS17.0 statistical software for rank sum test. $p < 0.05$ was significant.

## Results

*Pathological examination of nodules*

All the 10 nodules examined before treatment showed nuclear atypia, cell mitosis, which suggested that the inoculation modeling was successful: 1) Bodyweight growth curve: 2) Tumor weight and inhibition rate comparison between each group
*Pathological comparison of thymus tissue*
*Results of serum LDH AND HIF-1α, AST, ALT, AKP*

## Table 1. Primers in qRT-PCR Analysis of Gene Expression of Tumor Tissue

| Gene | Sense or antisense | Primer sequence |
|---|---|---|
| Bcl-2 | Sense primer | 5`GAC CTA GTA CCC ACT GAG ATT 3` |
| | Antisense primer | 5`CCA GAC ATT CGG AGA CCA 3` |
| Bax | Sense primer | 5`TTT TGC TTC AGG GTT TCA TC 3` |
| | Antisense primer | 5` GAC ACT CGC TCA GCT TCT TG 3` |
| β-actin | Sense primer | 5`GTG GAC ATC CGC AAA GAC 3` |
| | Antisense primer | 5`AAA GGG TGT AAC GCA ACT AA 3` |

## Table 2. Tumor Weight($\bar{x}\pm s$) and Tumor Inhibition rate

| Group | n | Weight of tumor (g) | Tumor inhibition rate |
|---|---|---|---|
| Model control group | 24 | 4.46±0.75 | |
| DDP control group | 24 | 1.66±0.22[b] | 62.70% |
| ASSF group | 24 | 2.51±0.38[b,c] | 43.70% |
| ASSF–DDP group | 24 | 1.29±0.23[b,c,d] | 71.00% |

## Table 3. Pathological Injury Score Comparison of Thymus Tissue

| Group | n | Pathological score of thymus tissue | | |
|---|---|---|---|---|
| | | 0 | 1 | 2 |
| Normal group | 16 | 15* | 1 | 0 |
| Model control group | 16 | 13* | 3 | 0 |
| DDP control group | 16 | 1 | 5 | 10 |
| ASSF group | 16 | 13* | 3 | 0 |
| ASS-DDP group | 16 | 8* | 7 | 1 |

*Compared with DDP control group, *p*<0.01(rank sum test); Because there are thymus pictures, so the editors may cancel this table 3 and relative notes

## Table 4a. Serum HIF-1α and LDH ($\bar{x}\pm s$, n=10)

| group | HIF-1α(pg/ml) | LDH (u/L) |
|---|---|---|
| Normal Control Group | 4.061±0.640 | 3999.35±295.55 |
| Model Control Group | 7.298±0.838[a] | 3631.56±262.03 |
| DDP Control Group | 3.443±1.159[b] | 7456.70±506.58[a,b] |
| AFSPG | 3.24±0.70[b] | 4049.39±246.04[c] |
| AFSP-DDPG | 3.57±1.09[b] | 4378.56±962.22[c] |

Compared with Normal Control Group, [a]*P*<0.01: compared with Model control group; [b]*P*<0.01: compared with DDP control group; [c]*P*<0.01

## Table 4b. Serum AST, ALT, AKP ($\bar{x}\pm s$, n=10)

| group | AKP(U/gprot) | AST(U/gprot) | ALT(U/gprot) |
|---|---|---|---|
| Normal Control Group | 2.174±0.536 | 57.104±14.688 | 64.148±21.917 |
| Model Control Group | 2.535±0.627[a] | 167.961±31.987[a] | 85.025±25.795[a] |
| DDP Control Group | 4.203±0.955[a,b] | 236.106±37.112[a,b] | 132.018±30.238[a,b] |
| AFSPG | 2.017±0.536[b,c] | 108.252±33.741[a,b,c] | 68.126±22.175[b,c] |
| AFSP-DDPG | 2.214±0.534[c] | 141.540±30.273[a,c] | 76.382±23.366[a,b,c] |

*Compared with Normal Control Group, [a]*P*<0.01; compared with Model control group, [b]*P*<0.01; compared with DDP control group, [c]*P*<0.01

**a**



**b**



## Figure 1. Bodyweight Growth Curve (n=12) of, 1a) Female Mice; 1b) Male Mice
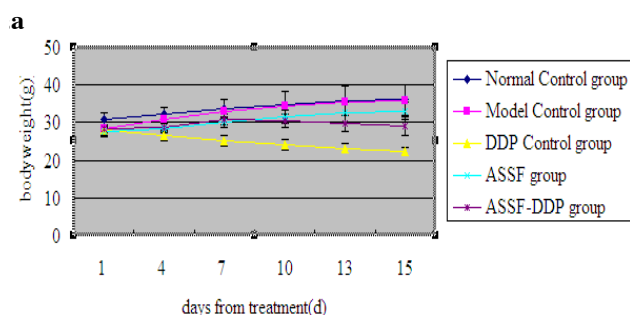
*The mean density and mean grey scale of mutant p53 in tumor tissue*
*The mean density and mean grey scale of caspase3 in tumor tissue*
*Relative expression of bcl-2 mRNA in the tumor tissue*
*Relative expression of of bax mRNA in the tumor tissue*

## Table 5. The Mean Density and Mean Grey Scale of Mutant p53 Protein in tumor tissue ($\bar{x}\pm s$, n=10)

| group | Mean density | Mean grey scale |
|---|---|---|
| Model control group | 0.335±0.008 | 118.980±3.181 |
| DDP control group | 0.282±0.010[b] | 133.270±3.048[b] |
| ASSF group | 0.302±0.011[b,c] | 128.270±2.047[b,c] |
| ASSF -DDPgroup | 0.280±0.012[b,d] | 139.811±3.126[b,d] |

Compared with model control group, [b]P<0.01; Compared with DDP control group, [c]P<0.01; Compared with ASSF group, [d]P <0.01. Protein expression are increased with the increase of mean density and decreased with the increase of mean grey scale

## Table 6. The Mean Density and Mean Grey Scale of Caspase3 in Tumor Tissue Expressed as ($\bar{x}\pm s$, n=10)

| group | Mean density | Mean grey scale |
|---|---|---|
| Model control group | 0.287±0.007 | 129.540±2.318 |
| DDP control group | 0.321±0.158[b] | 119.418±2.527 [b] |
| ASSF group | 0.310±0.106[b] | 122.443±2.676 [b,c] |
| ASSF -DDPgroup | 0.343±0.114[b,c,d] | 114.424±1.29 [b,c,d] |

*Compared with model control group, [b]P<0.01;compared with DDP control group, [c]P<0.01;compared with ASSF group, [d]P <0.01 .

## Table 7. Relative Expression of bcl-2 mRNA in tumor tissue

| group | β-actin (Ct value) | Bcl-2 (Ct value) | Bcl-2 (ΔCt) | ΔΔCt | 2-ΔΔCt |
|---|---|---|---|---|---|
| Model control group | 34.29 | 18.99 | 0.55 | 0 | 1 |
| DDP control group | 36.06 | 22.53 | 0.62 | 1.87 | 0.27 |
| ASSF group | 35.08 | 20.44 | 0.58 | 0.66 | 0.63 |
| ASSF-DDP group | 37.96 | 24.40 | 0.64 | 1.47 | 0.36 |

*The result indicated no obvious difference between DDP control group and ASSF-DDP group. 2-ΔΔCt indicated the relative times of bcl-2 mRNA of treatment group divided by that of model control group

## Table 8. Relative Expression of of Bax mRNA in the Tumor Tissue

| group | β-actin (Ct value) | Bax (Ct value) | Bax (ΔCt) | ΔΔCt | 2-ΔΔCt |
|---|---|---|---|---|---|
| Model control group | 34.35 | 25.05 | 0.72 | 0 | 1 |
| DDP group | 33.57 | 21.67 | 0.64 | -2.60 | 6.06 |
| ASSF group | 36.09 | 25.09 | 0.69 | -1.70 | 3.25 |
| ASSF-DDP group | 36.46 | 20.3 | 0.66 | -2.92 | 7.57 |

*Compared with model control group, [b]P<0.05. compared with DDP group, [c]P<0.05. 2-ΔΔCt indicated the relative times of bax mRNA of treatment group divided by that of model control group

A: Normal control group    B Model control group    C: DDP control group
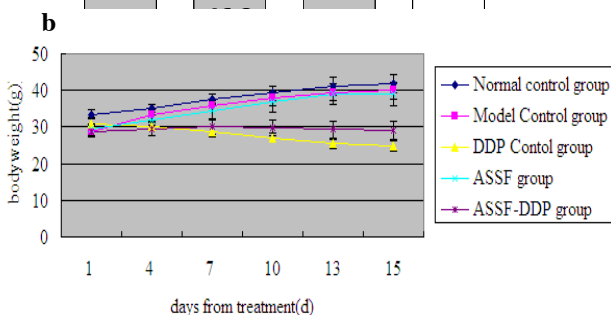


D: ASSF group    E: ASSF-DDP group
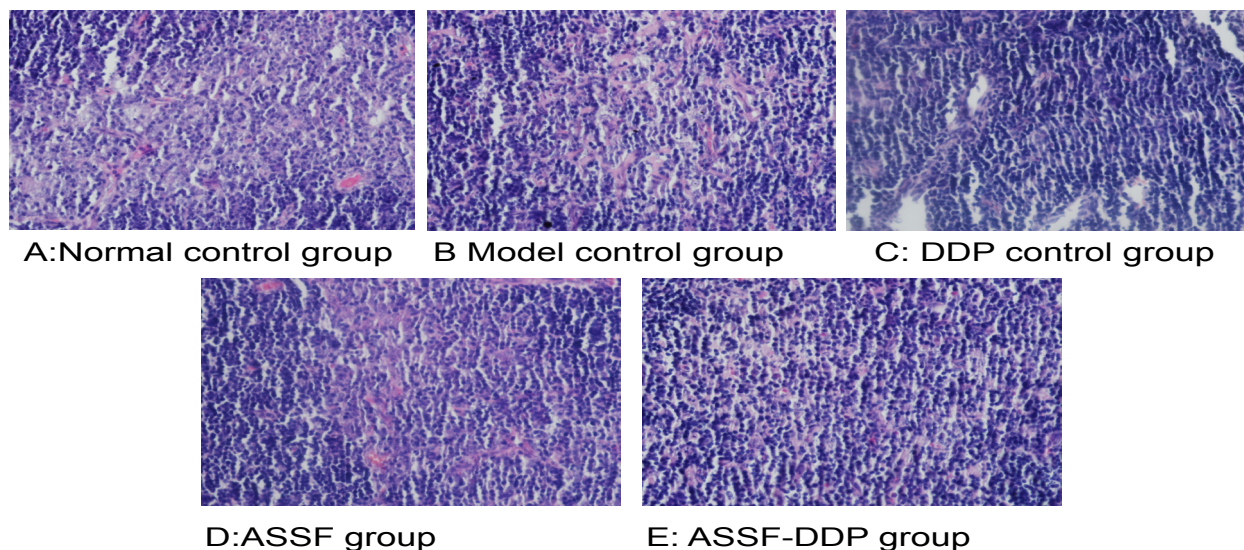
**Figure 2. Pathological Sections of Thymus tissue. A)** Normal group; **B)** Model control group; **C)** DDP control group; **D)** ASSF group; **E)** ASSF-DDPgroup. Thymocyte is red

**A) Model Control Group(40×10)**

**B) DDP Control Group(40×**



**C) ASSF group (40×10)**

**D) ASSF-DDP group(40×10)**
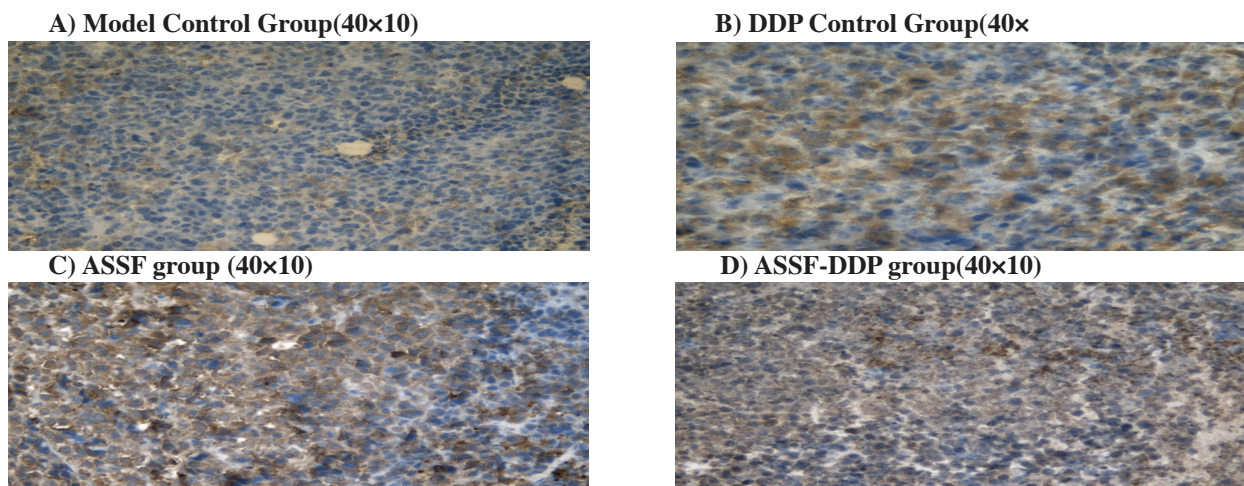


**Figure 3. Mutant P53 Expression in Tumor Tissue**

## Discussion

Hepatoma is currently one of the severe malignant diseases with the highest morbidity and mortality worldwide. DDP is the most commonly used chemical drug in the the comprehensive therapy of liver cancer, killing tumor cells mainly through DNA cross-linkage, which impedes cancer cell division, starts apoptotic signaling pathways. However, the clinical application of DDP is limited due to its serious toxic effects to normal cells, causing bone marrow suppression (Karima et al., 2012), liver injury (Bentli et al., 2013), gonad inhibition (García et al., 2012) , nephrotoxicity (Hoda et al., 2013), ototoxicity (Duval et al., 2012). Therefore, Chinese decoction combined with DDP has been applied in clinic, which can improve the therapeutic effects, reduce the clinical doses and toxic effects of DDP.

In traditional Chinese medicine, cancer occurs due to influent qi, blood and fluid stasis. Because stasis can produce accumulating heat and dampness, cancer is often treated through clearing heat and dampness, promoting blood circulation and removing blood stasis, resolving hard lump.

Angelica sinensis is sweet and warm, can nourish blood and make blood peaceful, dissolve blood stasis and produce fresh blood, so it can maintain good circulation and homeostasis, protect the normal function of the normal cells and kill the cancer cell by immune system and blood flow, reduce DDP-induced damage to the organs and tissues. Currently, extracts from Angelica sinensis possess anti-cancer and anti-oxidant activities, which activate the Nrf2 pathway to mediate the expression of many cellular anti-oxidative stress genes, protect organs and tissues against oxidative stress (Saw et al., 2013); extracts from Angelica sinensis can also suppress the growth of malignant brain tumor cells, up-regulate expression of p53 protein, cyclin kinase inhibitors p16, decrease the phosphorylation of Rb proteins, leading to arrest at the G0-G1 phase and activation of apoptosis-associated proteins in p53 pathway, significantly prolong patient survival (Lin et al., 2013). Angelica sinensis can decrease the adhesive, invasive and migratory ability of human lung adenocarcinoma A549 cells, down-regulate the expressions of matrix metalloproteinase-2 (MMP-2) and matrix metalloproteinase-9 (MMP-9) at both the protein and mRNA levels, inhibit the enzymatic activity of MMP-2 and MMP-9, possesses anti-growth and anti-metastasis activity against lung cancer cells (Gao et al.,

2012). Angelica sinensis polysaccharides can stimulate the human peripheral blood mononuclear cells (MNCs) to secret GM-CSF and IL-3 and protect the hematopoietic function of CD34(+) cells from myelosuppressive agent (Lee et al., 2012), induce CD34+CD38 cell senescence through up-regulation of p53, p16, p21, and Rb genes and repression of telomerase activity, effectively inhibit human acute myelogenous leukemia (AML) CD34+CD38 stem cell proliferation without suppressing normal hematopoietic stem and progenitor cells (Liu et al., 2013). Angelica Sinensis has clinical efficacy in treating radiotherapy-induced pneumonitis and fibrosis through down-expression of TNF-α and TGF-β1 both at mRNA and protein levels (Xie et al., 2006)

Radix sophorae flavescentis ait is bitter and cold in traditional Chinese medicine, can clear heat and eliminate dampness, kill parasite, promote urine to be formed, and treat accumulated lump in traditional Chinese medicine. Extracts from Radix sophorae flavescentis ait can inhibit tumor cell growth through up-regulation of caspase 3, down-regulation of bcl-2 at mRNA and protein levels (Wang et al., 2013). Matrine from Radix sophorae flavescentis can cause bid-mediated AIF nuclear translocation inducing caspase-independent apoptosis of human hepatocellular carcinoma cells (Zhou et al., 2014). Matrine can significantly inhibit the proliferation and promote the apoptosis of breast cancer MCF-7 cells in death receptor related pathway through up-regulation of Fas protein, supression of telomerase activity, down-regulation of VEGF protein resulting in inhibition of the tumor vascular formation (Li et al., 2013). Matrine can induce the activation of caspase-3 and -9 and the release of mitochondrial cytochrome C (Cyto C) to the cytosol. The upregulation of Bax and downregulation of Bcl-2 can cause apoptosis of human colon cancer cells in mitochondrial apoptotic pathway(Chang et al., 2013). Our previous Western blotting results showed matrine can inhibit the protein expression of bcl-2, VEGF, HDAC1 and increase the protein expression of bax, down regulate the ratio of bcl-2/bax, promoting apotosis of A549 cancer cells, inhibiting the proliferation of A549 cancer cells(Liu et al., 2014). Kuraridin and nor-kurarinone isolated from Sophora flavescens can also induce apoptosis of human gastric adenocarcinoma SGC-7901 cells(Rasul et al., 2011). The present study showed ASSF decoction could decrease P53, bcl-2 and increase bax and caspase-3 in the tumor of KM mice, which led to the apoptosis of tumor cells and inhibition of tumor growth.

Ionizing radiation and chemotheraputic drug both can cause hypoxia which further lead to higher expression of HIF-1α resulting in radioresistance and chemotherapy resistance of mice bearing xenografts (Song et al., 2014; Zhang et al., 2014). The present study showed ASSF decoction could decrease HIF-1α, which resulted in enhanced sensitivity of tumor cells to DDP.

Cisplatin depressed glutathione peroxidase and superoxide dismutase (SOD), resulted in increased leakage of LDH, AST, ALT, AKP, which could be attenuated by resveratrol extracted from herb (Valentovic, 2014). The increase in serum aldehyde dehydrogenase 1(LDH1) is correlated with poor prognosis such as higher pathologic grade and stage, as well as increased rate of recurrence (Hossein et al., 2014). The present study showed ASSF decoction could decrease high level of LDH, AST, ALT, AKP induced by DDP, reduce the toxicity of DDP to organs and tissues.

Caspase 3 and bax play important roles in inducing tumor cell apoptosis (Jung et al., 2014) , while mutant p53 and bcl-2 play important roles in inhibiting tumor cell apoptosis. Inducing tumor cell apoptosis is a good way for cancer theratpy. ASSF can increase caspase 3 and bax expression significantly, but cannot decrease p53 and bcl-2 to the same degree, which may be because ASSF plays strong roles in promoting expression of protein and mRNA, plays weak roles in inhibiting expression of molecules.

In this study, using KM mice inoculated hepatocarcinoma H22 cell line as model, we demonstrated that when ASSF was combined with DDP, the tumor inhibitory effect was significantly stronger than that when ASSF decoction or DDP was used alone.Our results suggest ASSF decoction combined with DDP could reduce the toxic effects of DDP and obtain better curative effects.

In conclusion, ASSF can inhibit tumor growth and has synergistic effect with DDP in treating tumor bearing mice. The synergistic effect may work through protection of thymus to make immune system function properly, decrease blood HIF-1α released by tumor tissue and may be correlated to the up-regulation of pro-apoptotic molecules such as caspase 3 and bax. ASSF can reduce serum LDH, AST (Palipoch et al., 2014), ALT (Palipoch et al., 2014), AKP whose increase might be related with DDP application

## Acknowledgements

## References

Bentli R, Parlakpinar H, Polat A, et al (2013). Molsidomine prevents cisplatin- induced hepatotoxicity. *Arch Med Res*, **44**, 521-8.

Chang C, Liu SP, Fang CH, et al (2013). Effects of matrine on the proliferation of HT29 human colon cancer cells and its antitumor mechanism. *Oncol Lett*, **6**, 699-704.

Chen H, Zhang J, Luo J, et al (2013). Antiangiogenic effects of oxymatrine on pancreatic cancer by inhibition of the NF-κB-mediated VEGF signaling pathway. *Oncol Rep*, **30**, 589-95.

Duval M, Daniel SJ (2012). Meta-analysis of the efficacy of

amifostine in the prevention of cisplatin ototoxicity. *J Otolaryngol Head Neck Surg*, **41**, 309-15.

Gao M, Zhang JH, Zhou FX, et al (2012). Angelica sinensis suppresses human lung adenocarcinoma A549 cell metastasis by regulating MMPs/TIMPs and TGF-β1. *Oncol Rep*, **27**, 585-93.

García MM, Acquier A, Suarez G, et al (2012). Cisplatin inhibits testosterone synthesis by a mechanism that includes the action of reactive oxygen species (ROS) at the level of P450scc. *Chem Biol Interact*. 199:185-91.

Hoda E. Mohamed, Sahar E. El-Swefy, et al (2013). Effect of erythropoietin therapy on the progression of cisplatin induced renal injury in rats. *Exp Toxicol Pathol*, **65** 197-203.

Hossein K, Elmira G, Mojgan A, et al (2014). ALDH1 in combination with CD44 as putative cancer stem cell markers are correlated with poor prognosis in urothelial carcinoma of the urinary bladder. *Asian Pac J Cancer Prev*, **15**, 2013-20.

Jin H, Sun Y, Wang S, et al (2013). Matrine sctivates PTEN to induce growth inhibition and apoptosis in V600EBRAF harboring melanoma cells. *Int J Mol Sci*, **14**, 16040-57.

Jung HI, Jo MJ, Kim HR, et al (2014). Extract of *Saccharina japonica* induces apoptosis companied by cell cycle arrest and endoplasmic reticulum stress in SK-Hep1 human hepatocellular carcinoma cells. *Asian Pac J Cancer Prev*, **15**, 2993-9.

Lee JG, Hsieh WT, Chen SU, Chiang BH (2012). Hematopoietic and myeloprotective activities of an acidic Angelica sinensis polysaccharide on human CD34+ stem cells. *J Ethnopharmacol*, **139**, 739-45.

Lee YY, Mok MT, Cheng AS (2014). Dissecting the pleiotropic actions of HBx mutants against hypoxia in hepatocellular carcinoma. *Hepatobiliary Surg Nutr*, **3**, 95-7.

Li HJ, Wang JM, Tian YT, et al (2013). Effect of matrine on Fas, VEGF, and activities of telomerase of MCF-7 cells. *Zhongguo Zhong Xi Yi Jie He Za Zhi*, **33**, 1247-51.

Lin YL, Lai WL, Harn HJ, et al (2013). The methanol extract of *Angelica sinensis* induces cell apoptosis and suppresses tumor growth in human malignant brain tumors. *Evid Based Complement Alternat Med*, **2013**, 394636.

Liu J, Xu CY, Cai SZ, et al (2013). Senescence effects of *Angelica sinensis* polysaccharides on human acute myelogenous leukemia stem and progenitor cells. *Asian Pac J Cancer Prev*, **14**, 6549-56.

Liu S, Cao M, Li D, et al (2011). Purification and anticancer activity investigation of pentacyclic triterpenoids from the leaves of Sinojackia sarcocarpa L.Q. Luo by high-speed counter-current chromatography. *Nat Prod Res*, **25**, 1600-6.

Liu Y, Li Y, Qin J, et al (2014). Matrine reduces proliferation of human lung cancer cells by inducing apoptosis and changing miRNA expression profiles. *Asian Pac J Cancer Prev*, **15**, 2169-77.

Lovine B, Oliviero G, Garofalo M, et al(2014). The Anti-Proliferative Effect of L-Carnosine Correlates with a Decreased Expression of Hypoxia Inducible Factor 1 alpha in Human Colon Cancer Cells. *PLoS One*, **9**, 96755.

Palipoch S, Punsawad C, Koomhin P, et al (2014). Hepatoprotective effect of curcumin and alpha-tocopherol against cisplatin-induced oxidative stress. *BMC Complement Altern Med*, **14**, 111.

Pu LP, Chen HP, Cao MA, et al(2013). The antiangiogenic activity of Kushecarpin D, a novel flavonoid isolated from *Sophora flavescens* Ait. *Life Sci*, **93**, 791-7.

Rasul A, Yu B, Yang LF, et al (2011). Induction of mitochondria-mediated apoptosis in human gastric adenocarcinoma SGC-7901 cells by kuraridin and Nor-kurarinone isolated from Sophora flavescens. *Asian Pac J Cancer Prev*, **12**, 2499-504.

Rjiba-Touati K, Ayed-Boussema I, Skhiri H, et al (2012).

Induction of DNA fragmentation, chromosome aberrations and micronuclei by cisplatin in rat bone-marrow cells: Protective effect of recombinant human erythropoietin . *Mutat Res*, **747**, 202-6.

Saw CL, Wu Q, Su ZY, et al (2013). Effects of natural phytochemicals in Angelica sinensis (Danggui) on Nrf2-mediated gene expression of phase II drug metabolizing enzymes and anti-inflammation. *Biopharm Drug Dispos*, **34**, 303-11.

Song HY, Deng XH, Yuan GY, et al (2014). Expression of bcl-2 and p53 in induction of esophageal cancer cell apoptosis by ECRG2 in combination with cisplatin. *Asian Pac J Cancer Prev*, **15**, 1397-401.

Song K, Li M, Xu XJ, et al (2014). HIF-1α and GLUT1 gene expression is associated with chemoresistance of acute myeloid leukemia. *Asian Pac J Cancer Prev*, **15**, 1823-9.

Valentovic MA, Ball JG, Brown JM, et al (2014). Resveratrol attenuates cisplatin renal cortical cytotoxicity by modifying oxidative stress. *Toxicol In Vitro*, **28**, 248-57.

Wang Y, Han C, Fang X, et al (2013). Effect of Kushen (*Radix Sophorae flavescentis*) extract on laryngeal neoplasm Hep2 cells. *J Tradit Chin Med*, **33**, 218-22.

Yu Hui-Min, Wang Tsing-Cheng (2012). Mechanism of cisplatin resistance in human urothelial carcinoma cells. *Food Chem Toxicol*, **50**, 1226-37.

Xie CH, Zhang MS, Zhou YF, et al (2006). Chinese medicine Angelica sinensis suppresses radiation-induced expression of TNF-alpha and TGF-beta1 in mice. *Oncol Rep*, **15**, 1429-36.

Zhang HM, Wang XY, Wang XM, et al (2012). Inhibition of Lycium barbarum polysaccharide on transplanted liver cancer in mice. *Chinese Traditional Herbal Drugs*, **43**, 1142-6.

Zhang YS, Jiang G, Gao H, et al (2014). Influence of ionizing radiation on ovarian carcinoma SKOV- 3 xenografts in nude mice under hypoxic conditions. *Asian Pac J Cancer Prev*, **15**, 2353-8.

Zhou H, Xu M, Gao Y, et al (2014). Matrine induces caspase-independent program cell death in hepatocellular carcinoma through bid-mediated nuclear translocation of apoptosis inducing factor. *Mol Cancer*, **13**, 59.